Figure 1. (a) The plasma concentration-time plots of pilsicainide from patients who received the intravenous infusion of the drug. For simplicity, the data obtained after 360 minutes postdose were truncated. The inset shows the complete data set. (b) Scatter plots of the observed plasma pilsicainide concentrations versus those predicted by the final population pharmacokinetic (PK) model. The line represents that of unity (y = x). (c) Scatter plots of weighted residuals as a function of the final PK model-predicted plasma drug concentrations. Detailed descriptions of the population PK analysis are given in text.

shape parameter ( ); and the interindividual and residual variabilities in each conduction parameter. Using sequential population PK/PD analysis with the effect compartment model, we successfully accomplished the analysis for PK/PD data with hysteresis. Age and the development of the ST-segment elevation were significant covariates for the K_{eo} of QRS, but clinical implications of these findings remain unclear. While the correlation between the observed and predicted PD responses was not very strong as compared with that between observed and predicted plasma drug concentrations in the PK analysis, prediction of PD responses by the population PD model was considered unbiased. As a typical example, Figure 2 shows the relationship between the observed prolongation of PEQ interval (PEQ) and that predicted by the model (Figure 2a) and the weighted residual plots as a function of predicted drug concentrations (Figure 2b). The data for other PD parameters are shown only in numerical values (Table III). The multivariate analysis revealed that patients developing the drug-induced ST-segment elevation (responders) would have 50% and 40% higher E_{max} values for PEQ (Figure 3) and PQ, respectively, than the nonresponders would (P < .01).

DISCUSSION

The present study is the first to perform a population PK/PD analysis of the class IC antiarrhythmic agent pilsicainide in patients with cardiac arrhythmias. The population PK analysis demonstrates that gender and CL_{cr} are independent covariates of the interindividual variability of body-weight-normalized CL of the drug. As shown in Table II, the relationships between CL_{cr} and CL of pilsicainide predicted by the population PK model in male and female patients are clearly different, and female patients have on average 50% lower systemic CL of the drug than do male patients irrespective of body weight and CL_{cr}. There was no statistically significant difference in patients' background between men and women except for body size (ie, total body weight and height). Our data suggest that both gender and CL_{cr} may be important clinical covariates for individualizing doses of pilsicainide during chronic administration. The present study warrants further clinical studies to confirm these findings during long-term administration of the drug.

The finding that the systemic CL of pilsicainide correlates positively with predicted CL_{cr} may be explained by the PK characteristics of the drug. After intravenous administration, >90% of the dose is eliminated primarily via the kidneys into urine in unchanged form in young healthy subjects.[3,8] The mean PK parameters (ie,

108

Table II Final Population Pharmacokinetic Model Formulated Based on
Data Obtained From 91 Patients After Intravenous Administration of Pilsicainide

Parameter Symbol	Annotation	Value	SE
Fixed effects[a]			
$_1$, L/min/kg	CCR coefficient in Fac	3.28	0.582
$_2$	Female coefficient in clearance	0.498	0.0681
V_c, L/kg	Volume of central compartment	0.0775	0.0190
Q, L/min	Intercompartmental clearance	1.73	0.318
$_3$, L/kg	Intercept of volume of peripheral compartment	0.783	0.119
$_4$	AGE coefficient in volume of peripheral compartment	0.00627	0.00190
Random effects[b]			
$_{CL}^2$	Interindividual variance of CL_j	0.0198	0.0182
$_{Vc}^2$	Interindividual variance of V_{cj}	0.101	0.118
$_Q^2$	Interindividual variance of Q_j	0.175	0.0811
$_{Vp}^2$	Interindividual variance of V_{pj}	0.0635	0.0168
$_2$	Intraindividual variance of C_{ij}	0.0339	0.00888

SE = standard error of mean for estimation; CCR = predicted creatinine clearance (L/min/kg); AGE = age (years); CL_{TV} = typical value of clearance (CL) in the population (L/min/kg); SEX = 0 for male and 1 for female; V_{pTV} = typical value of volume of peripheral compartment (V_p) in the population (L/kg); P_j = estimated pharmacokinetic parameter in the jth individual; P_{TV} = typical value of a pharmacokinetic parameter in the population; P_j = jth interindividual variability in P_{TV}; C_{ij} and $C_{pred, ij}$ = jth observed and estimated plasma concentrations of pilsicainide in the jth individual, respectively; $_{ij}$ = jth residual variability in plasma concentration of pilsicainide in the jth individual.
a. Fac = $_1$ • CCR; CL_{TV} = Fac • (1 − SEX) + $_2$ • Fac • SEX; V_{pTV} = $_3$ + $_4$ • AGE.
b. P_j = P_{TV} • (1 + P_j); C_{ij} = $C_{pred, ij}$ • (1 + $_{ij}$).

CL, V_p estimated by our population PK analysis (Figure 1, Table II) agree well with those reported in the conventional PK studies.[3,6,13] The reason female patients possess significantly ($P < .01$) lower body-weight-normalized CL than male patients do (Table II) remains unclear. However, we are tempted to speculate that a gender difference in the activity of certain unidentified renal OCTs may be associated with our finding. Involvement of active renal tubular secretion of the drug has been strongly suggested by previous studies[3,6,13] because the renal CL of pilsicainide is approximately 2 times greater than creatinine clearance in healthy subjects. Shiga et al[8] demonstrated that the renal elimination of pilsicainide is interfered with significantly by the coadministration of cimetidine, which has been shown to inhibit active tubular excretion of various cationic drugs (eg, procainamide[14] and metformin[15]). Since pilsicainide is a cationic compound, certain OCTs may be involved in its renal elimination. To our knowledge, no data are available on whether gender difference exists in the OCT activities in human renal tubular cells. However, previous studies[16-19] demonstrated that female rats have a substantially lower OCT activity for tetraethyl ammonium and other cationic small molecules and lower level of mRNA expression of OCT2, but not of OCT1, than male rats in renal tubular cells. Similarly, the activity of the renal organic anion transporter (OAT) in female rats is

also significantly less than in male rats.[20,21] Recently, female patients have been shown to have a 50% less systemic CL of telmisartan, an angiotensin II receptor antagonist, than do male patients.[22] The drug and its conjugate are claimed to be excreted primarily into bile via an OAT, canalicular multispecific OAT.[23]

The sequential population PK/PD analysis using the effect compartment model revealed that the patients who exhibited a BrS-like ECG pattern (coved or saddle-back ST-segment elevation >1.5 mV) after pilsicainide administration (responders) also showed significantly ($P < .01$) greater prolongation of PQ and PEQ intervals compared to those who did not exhibit the ECG pattern (nonresponders). E_{max} values of PQ and PEQ in the responders were 40% and 50%, respectively, greater than those in the nonresponders (Table III, Figure 3). These findings are consistent with previous studies[5,7,24,25] conducted in patients diagnosed with BrS based on ECG responses elicited by the administration of various class I antiarrhythmics (flecainide, disopyramide, and mexiletine), using similar diagnostic criteria as employed in the present study. Our data suggest that pilsicainide-induced ST-segment elevations mimicking BrS and greater prolongation of intracardiac conduction may be attributable to exaggerated responsiveness of sodium channels to pilsicainide. Since BrS is a sodium channelopathy, these parameters may serve as useful tools for probing

109

Table III Final Population Pharmacodynamic Model for the Relationship Between Effect Site Pilsicainide Concentrations and Electrocardiogram Parameters Associated With Intracardiac Conduction (n = 77)

Pharmacodynamic Parameter	P	PQ	PEQ	QRS
Number of pharmacodynamic data points	296	296	296	352
Error model				
Interindividual	Proportional	Additive	Proportional	Proportional
Residual	Additive	Proportional	Additive	Proportional
OBJ	18.428	54.971	12.101	81.604
Fixed effects				
K_{e0TV}, min^{-1}	0.330 (0.0981)	0.0756 (0.0118)	0.130 (0.0609)	0.0108 (0.0321)
K_{e0TV} + /AGE	—	—	—	1.33 (2.08)
$K_{e0TV} \cdot (1 - STE) + \cdot K_{e0TV} \cdot STE$	—	—	—	9.67 (4.20)
E_{maxTV}, ms	46.6 (16.1)	73.2 (11.2)	26.2 (9.37)	26.4 (24.7)
$E_{maxTV} + \cdot AGE$	—	—	—	3.58 (0.324)
$E_{maxTV} \cdot (1 - SEX) + \cdot E_{maxTV} \cdot SEX$	—	1.34 (0.156)	—	1.55 (0.282)
$E_{maxTV} \cdot (1 - STE) + \cdot E_{maxTV} \cdot STE$	—	1.38 (0.135)	1.48 (0.237)	—
EC_{50TV}, µg/mL	13.7 (13.0)	4.19 (1.31)	0.675 (0.354)	4.97 (11.0)
$EC_{50TV} + \cdot AGE$	−0.174 (0.167)	−0.0504 (0.0181)	—	—
TV	0.577 (0.111)	0.828 (0.0663)	1.61 (1.25)	0.658 (0.173)
Random effects				
$^2_{Ke0}$	9.59 (8.70)	2.18E-9 (0.00183)	1.12 (0.988)	25.1 (12.0)
$^2_{Emax}$	0.347 (0.160)	743 (438)	0.370 (0.100)	0.361 (0.566)
$^2_{EC50}$	1.66E-8 (2.50)	0.468 (0.574)	1.34E-8 (0.132)	9.06E-5 (3.54)
^{2}	0.294 (0.218)	0.215 (0.127)	0.382 (0.978)	0.343 (0.336)
^{2}	40.4 (10.6)	0.0503 (0.0136)	53.0 (10.5)	0.140 (0.0378)

Data are presented as population mean (SE). OBJ = decrement of objective function value from basic model; K_{e0TV}, E_{maxTV}, EC_{50TV}, and TV = the typical values of effect site elimination rate constant (min^{-1}), maximum effect (ms), effect site pilsicainide concentrations associated with a 50% E_{max} (µg/mL), and shape parameter (ie, Hill coefficient) in the patient population; ^2_x = the interindividual variance of each parameter; ^{2} = the residual variance of pharmacodynamic response; AGE = age (years); STE = 0 for nonresponder and 1 for responder about >0.15 mV ST-segment elevation after intravenous pilsicainide administration; SEX = 0 for male and 1 for female; SE = standard error of mean for estimation.

sodium channel function in patients who have arrhythmias suspected of BrS.

Our data should be interpreted with caution because of the limitations described below. First, our patients were not homogenous regarding demographic and clinical backgrounds. For instance, patients with atrial fibrillation (group C) were significantly older and had lower CL_{cr} compared to those suspected of BrS (groups A and B, Table I). In addition, female patients were more prevalent (36%) in the atrial fibrillation group than in groups A and B (16%). Since we analyzed the population PK of pilsicainide by incorporating age, CL_{cr}, and gender as independent covariates, we consider that our conclusion would be tenable for the bias associated with patient heterogeneity described above. Nevertheless, we cannot categorically deny the possibility that atrial fibrillation has a unique effect on the PK of pilsicainide independent of age, CL_{cr}, and gender. In this context, further studies are required to clarify this issue. Second, because the number of patients who participated in our population PK and PD study was relatively small, it was not feasible to undertake model validation to assess stability and performance using a data-splitting method. Thus, further studies are necessary to confirm our findings using a larger number of subjects. Finally, there are fundamental difficulties in the accurate diagnosis of BrS. All patients who participated in the present study had a family history of cardiac sudden death, syncope episodes, and right bundle branch block coupled with typical or marginal ST-segment elevations in ECG at rest despite structurally normal hearts. ST-segment elevation of >+0.15 or +0.20 mV after the administration of class I antiarrhythmic agents has been proposed as a diagnostic criterion of BrS,[7] while its sensitivity and specificity remain to be confirmed by a large clinical trial. While many genetic mutations of SCN5A have been implicated in the arrhythmogenicity of BrS,[26-28] such mutations are detected in at most 20% of the patients who met the above diagnostic criteria of BrS.[29,30] Therefore, caution must
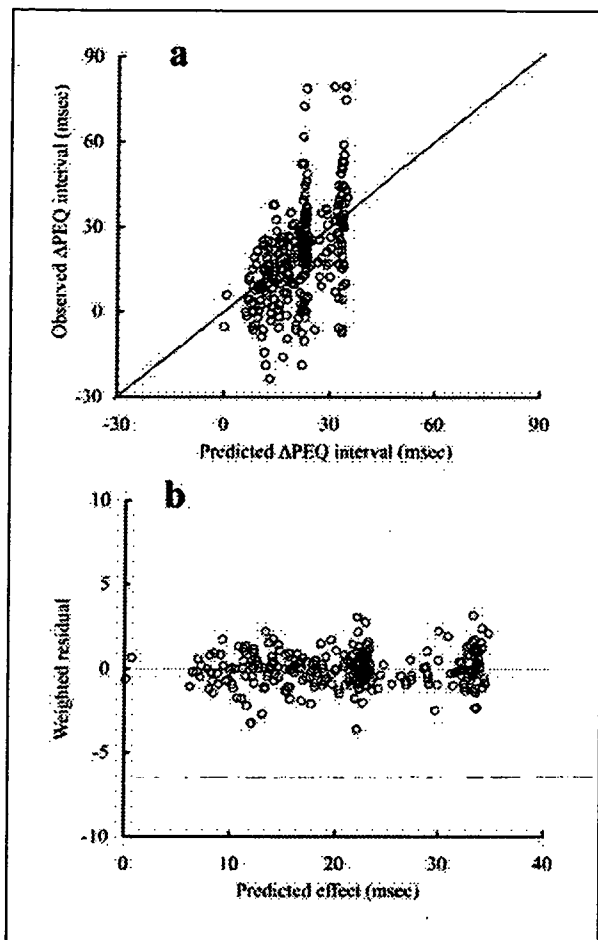
110

Figure 2. (a) Scatter plots of the observed PEQ interval versus the interval predicted by the final population PK/PD model, with reference to the line of unity (y = x). (b) Scatter plots of weighted residuals of the PEQ interval versus the final population PK/PD model-predicted values.
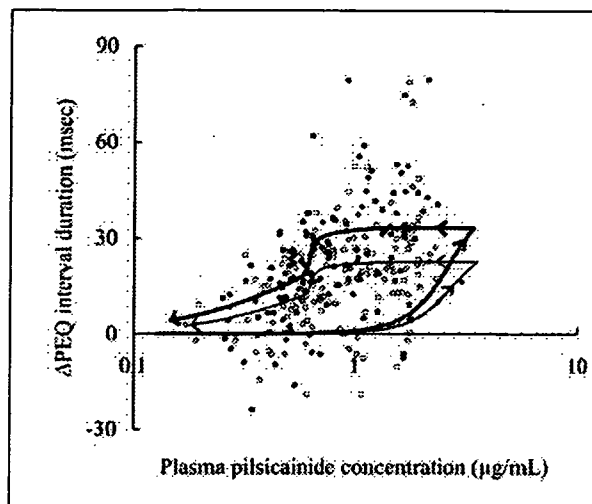

Figure 3. Relationships between plasma pilsicainide concentrations and prolongation of PEQ interval relative to the baseline values (ie, PEQ) in patients after intravenous infusion of pilsicainide. Thick and thin curves represent the typical plasma drug concentration-response relationship with time-sequence depicted by arrows in the patients who developed the exaggerated ST-segment elevation (●) and those who did not (O). Note that the phenotypic trait of the ST-segment elevation >0.15 mV from the baseline tracing is a significant (P < .05) covariate for the maximum prolongation of PEQ (E_{max}). Detailed descriptions of the population PK/PD analysis are given in the text.

be exercised in interpreting our data in the light of diagnostic usefulness, particularly in association with genetic mutations of SCN5A, until a more satisfactory method for molecular diagnosis of BrS becomes available.

In conclusion, we have performed a population PK analysis of the pure sodium channel blocker pilsicainide in patients with cardiac arrhythmias. We found that gender and CL_{cr} are independent covariates associated with systemic clearance of the drug. The population PD analysis revealed that the patients who developed BrS-like ST-segment elevation after the administration of pilsicainide also have a greater

dromotropic effect in PQ and PEQ intervals than those who did not. Our data further support the idea that ST-segment elevations observed in patients with BrS may be associated with greater susceptibility of sodium channels to class IC antiarrhythmics.

The authors are grateful to Mr Atsushi Watanabe and Miss Asako Nishi for excellent technical assistance and also thank the clinical staff in the Department of Cardiology, St Marianna University School of Medicine, for clinical collaboration. There are no conflicts of interest associated with this work.

REFERENCES

1. Hattori Y, Inomata N, Aisaka K, Ishihara T. Electrophysiological actions of N-(2, 6-dimethylphenyl)-8-pyrrolizidine-acetamide hydrochloride hemihydrate (SUN1165), a new antiarrhythmic agent. J Cardiovasc Pharmacol. 1986;8:998-1002.

2. Hattori Y, Inomata N. Modes of the Na channel blocking action of pilsicainide, a new antiarrhythmic agent, in cardiac cells. Jpn J Pharmacol. 1992;58:365-373.

3. Nakashima M, Kanamaru M. Phase I study of pilsicainide hydrochloride (SUN1165) injection. J Clin Ther Med. 1998;14:47-61.

4. Antzelevitch C, Brugada P, Borggrefe M, et al. Brugada syndrome: report of the second consensus conference. Circulation. 2005;111:659-670.

111

5. Miyazaki T, Mitamura H, Miyoshi S, Soejima K, Ogawa S, Aizawa Y. Autonomic and antiarrhythmic drug modulation of ST segment elevation in patients with Brugada syndrome. *J Am Coll Cardiol.* 1996;27:1061-1070.

6. Scheiner LB, Rosenberg B, Marathe VV. Estimation of population characteristics of pharmacokinetic parameters from routine clinical data. *J Pharmacokinet Biopharm.* 1977;5:445-479.

7. Brugada R, Brugada J, Antzelevitch C, et al. Sodium channel blockers identify risk for sudden death patients with ST-segment elevation and right bundle branch block but structurally normal hearts. *Circulation.* 2000;101:510-515.

8. Shiga T, Hashiguchi M, Urae A, Kasanuki H, Rikihisa T. Effect of cimetidine and probenecid on pilsicainide renal clearance in humans. *Clin Pharmacol Ther.* 2000;67:222-228.

9. Cockcroft DW, Gault MH. Prediction of creatinine clearance from serum creatinine. *Nephron.* 1976;16:31-41.

10. Parke J, Holford NH, Charles BG. A procedure for generating bootstrap samples for the validation of nonlinear mixed-effects population models. *Comput Methods Programs Biomed.* 1999;59:19-29.

11. Sheiner LB, Stanski DR, Vozeh S, Miller RD, Ham J. Simultaneous modeling of pharmacokinetics and pharmacodynamics: application to d-tubocurarine. *Clin Pharmacol Ther.* 1979;25:358-371.

12. Ailings M, Wilde A. Brugada syndrome: clinical data and suggested pathophysiological mechanism. *Circulation.* 1999;99:666-673.

13. Konishi T, Bito K, Matsumura T, Kanamaru M. The clinical pharmacokinetics and antiarrhythmic effect of intravenous pilsicainide hydrochloride [SUN1165 (inj)]. *J Clin Ther Med.* 1998;14:107-121.

14. Somogyi A, McLean A, Heinzow B. Cimetidine-procainamide pharmacokinetic interaction in man: evidence of competition for tubular secretion of basic drugs. *Eur J Clin Pharmacol.* 1983;25:339-345.

15. Somogyi A, Stockley C, Keal J, Rolan P, Bochner F. Reduction of metformin renal tubular secretion by cimetidine in man. *Br J Clin Pharmacol.* 1987;23:545-551.

16. Kleinman LI, Lowenstein MS, Goldstein L. Sex difference in the transport of p-aminohippurate by the rat kidney. *Endocrinology.* 1966;78:403-406.

17. Bowman HM, Hook JB. Sex differences in organic ion transport by rat kidney. *Proc Soc Exp Biol Med.* 1972;141:258-262.

18. Urakami Y, Nakamura N, Takahashi K, et al. Gender differences in expression of organic cation transporter OCT2 in rat kidney. *FEBS Lett.* 1999;461:339-342.

19. Urakami Y, Okuda M, Saito H, Inui K. Hormonal regulation of organic cation transporter OCT2 expression in rat kidney. *FEBS Lett.* 2000;473:173-176.

20. Reyes JL, Melêndez E, Alegría A, Jaramillo-Juarez F. Influence of sex differences on the renal secretion of organic anions. *Endocrinology.* 1998;139:1581-1587.

21. Kato Y, Kuge K, Kusuhara H, Meier PJ, Sugiyama Y. Gender difference in the urinary excretion of organic anions in rats. *J Pharmacol Exp Ther.* 2003;302:483-489.

22. Micardis (telmisartan) [product information]. Ridgefield, Conn: Boehringer Ingelheim Pharmaceuticals; 1998.

23. Nishino A, Kato Y, Igarashi T, Sugiyama Y. Both cMOAT/MRP2 and another unknown transporter(s) are responsible for the biliary excretion of glucuronide conjugate of the nonpeptide angiotensin II antagonist, telmisartan. *Drug Metab Dispos.* 2000;28:1146-1148.

24. Shimizu W, Antzelevitch C, Suyama K, et al. Effect of sodium channel blockers on ST segment, QRS duration, and corrected QT interval in patients with Brugada syndrome. *J Cardiovasc Electrophysiol.* 2000;11:1320-1329.

25. Takenaka S, Kusano KF, Hisamatsu K, et al. Relatively benign clinical course in asymptomatic patients with Brugada-type electrocardiogram without family history of sudden death. *J Cardiovasc Electrophysiol.* 2001;21:2-6.

26. Chen Q, Kirsch GE, Zhang D, et al. Genetic basis and molecular mechanism for idiopathic ventricular fibrillation. *Nature.* 1998;392:293-296.

27. Vatta M, Dumaine R, Varghese G, et al. Genetic and biophysical basis of sudden unexplained nocturnal death syndrome (SUNDS), a disease allelic to Brugada syndrome. *Hum Mol Genet.* 2002;11:337-345.

28. Vatta M, Dumaine R, Antzelevitch C, et al. Novel mutations in domain I of SCN5A cause Brugada syndrome. *Mol Genet Metab.* 2002;75:317-324.

29. Towbin JA. Molecular genetic basis of sudden cardiac death. *Cardiovasc Pathol.* 2001;10:283-295.

30. Brugada R, Roberts R. Genetic aspects of arrhythmias. *Am J Med Genet.* 2000;97:310-318.

112

Functional characterization of *SLCO1B1* (*OATP-C*) variants, *SLCO1B1*5*, *SLCO1B1*15* and *SLCO1B1*15 + C1007G*, by using transient expression systems of HeLa and HEK293 cells

Yoshio Kameyama[a,b], Keiko Yamashita[a], Kaoru Kobayashi[a], Masakiyo Hosokawa[a] and Kan Chiba[a]

Objectives *SLCO1B1*5* and *SLCO1B1*15* have been reported to reduce the clearance of pravastatin in healthy volunteers. However, there remains controversy in the effects of *SLCO1B1*5* on the activity of OATP1B1 *in vitro*. In addition, the effect of *SLCO1B1*15* on the function of OATP1B1 has not been studied using cDNA-expression systems. Object of the present study was to study the influence of *SLCO1B1*5*, **15* and **15 + C1007G*, a novel haplotype found in a patient with pravastatin-induced myopathy, on the functional properties of OATP1B1 by transient expression systems of HEK293 and HeLa cells using endogenous conjugates and statins as substrates.

Methods Transporting assays for endogenous substrates were performed using tritium labeled estradiol-17β-D-glucuronide and estrone-3-sulfate. Quantitation of pravastatin, atorvastatin, cerivastatin and simvastatin were carried out using HPLC tandem mass spectrometry.

Results The transporting activities of cells expressing *SLCO1B1*5*, **15* and **15 + C1007G* decreased significantly but those of *SLCO1B1*1b*, **1a + C1007G* and **1b + C1007G* were not altered for all of the substrates tested except for simvastatin. Kinetic analysis of pravastatin and atorvastatin showed that K_m values were not altered but V_{max} values decreased significantly in cells expressing *SLCO1B1*5*, **15* and **15 + C1007G*. Immunocytochemical study showed that *SLCO1B1*5*,

*15 and **15 + C1007G* proteins are localized not only at the plasma membrane but also in the intracellular space.

Conclusions These findings suggest that *521T > C*, existing commonly in *SLCO1B1*5*, **15* and **15 + C1007G*, is the key single nucleotide polymorphism (SNP) that determines the functional properties of *SLCO1B1*5*, **15* and **15 + C1007G* allelic proteins and that decreased activities of these variant proteins are mainly caused by a sorting error produced by this SNP. *Pharmacogenetics and Genomics* 15:513-522 c 2005 Lippincott Williams & Wilkins.

Introduction

For hepatic eliminating drugs, uptake into hepatocytes from the portal vein is a prerequisite step for subsequent metabolism and/or biliary excretion. Many transporters are expressed at the basolateral membrane of hepatocytes, such as organic anion-transporting polypeptides, organic anion transporters, organic cation transporters and sodium-dependent taurocholate transporting polypeptide [1]. Among them, OATP1B1 (gene, *SLC21A6/SLCO1B1*), also known as OATP-C, liver specific transporter-1 [2] or OATP2 [3], plays a crucial role in the hepatic uptake of a variety of structurally divergent compounds [4]. OATP1B1 can transport endogenous and a wide variety of exogenous substances, such as pravastatin [3], benzylpenicillin [5], bromosulfophtalein [6], [D-penicil-

lamine[2,5]]enkephalin, BQ-123 [7], methotrexate [8], rifampicin [9], cerivastatin [10] and rosuvastatin [11]. Accordingly, genetic polymorphisms of *SLCO1B1* could give rise to remarkable alteration of pharmacokinetics of certain drugs if they are substrates of this transporter.

Tirona *et al.* [8] first reported 16 single nucleotide polymorphisms (SNPs) and haplotypes designated as *SLCO1B1*1b* to **14* and the effects of those variant alleles on the transporting activity of OATP1B1 determined by using a transient expression system of HeLa cells. They found that six of these variant alleles, including *SLCO1B1*5*, reduced the transporting activity of OATP1B1 for estradiol-17β-D-glucuronide and estrone-3-sulfate to less than 50% of that in the case of

*SLCO1B1*1a* (reference allele). Based on their findings, they suggested that *SLCO1B1*5* represents a heretofore unrecognized factor influencing drug disposition since the frequency of this allele is relatively high in European-Americans [8]. In accordance with their suggestion, Mwinyi *et al.* [12] recently reported that *SLCO1B1*5* remarkably decreased the non-renal clearance of pravastatin in Caucasian subjects. Contradicting these findings, however, Nozawa *et al.* [13] reported that *SLCO1B1*5* did not alter the transporting activity of OATP1B1 for estrone-3-sulfate when it was expressed in HEK 293 cells. Therefore, controversy remains regarding the effects of this variant allele on the activity of OATP1B1. On the other hand, in the same report, Nozawa *et al.* [13] also described a novel haplotype of *SLCO1B1* possessing 388A > G in addition to the mutation of *SLCO1B1*5* (521T > C), which is designated *SLCO1B1*15*. Since the frequency of this allele is relatively high in the Japanese population [13], this variant allele of *SLCO1B1* could represent a factor influencing drug disposition in Japanese or other Asian subjects. In fact, Nishizato *et al.* [14] subsequently reported that *SLCO1B1*15* significantly reduced non-renal clearance of pravastatin in Japanese subjects. However, there have been no reports on the effect of *SLCO1B1*15* on the transporting activity of OATP1B1 determined by using a cDNA expression system.

In the present study, we examined the effects of *SLCO1B1*5* and *15* on the functional properties of OATP1B1 using transiently expressed systems of HeLa and HEK293 cells with typical substrates of OATP1B1, estradiol-17β-D-glucuronide and estrone-3-sulfate. We also examined the effects of *SLCO1B1*15* + *C1007G*, an allele possessing 1007C > G in addition to the mutation of *SLCO1B1*15* (388A > G and 521T > C), which was found in a Japanese patient with hypercholesterolemia who experienced muscle pain and loss of muscle strength after taking pravastatin. In addition, we studied the effects of these variant alleles on the transporting activity of OATP1B1 for pravastatin, atorvastatin, cerivastatin and simvastatin using a HPLC tandem mass spectrometry. Moreover, the effects of these variant alleles on the intracellular localization of OATP1B1 protein in HeLa and HEK293 cells were also studied.

Methods

Reagents

[^{3}H]-Estrone-3-sulfate ammonium salt (1702 GBq/mmol) and [^{3}H]-estradiol-17β-D-glucuronide (1498.5 and 1665 GBq/mmol) were purchased from PerkinElmer Life Science, Inc. (Boston, Massachusetts, USA). Zero Blunt TOPO PCR Cloning Kit and pcDNA3.1/Zeo were obtained from Invitrogen (Carlsbad, California, USA). Pravastatin, atorvastatin, cerivastatin and simvastatin were kindly donated by Sankyo Co. (Tokyo, Japan).

Rabbit anti-human LST-1 (OATP1B1) antibody was purchased from Alpha Diagnostic International, Inc. (San Antonio, Texas, USA). All other reagents were commercially available and of reagent grade. HEK293 cells were purchased from Health Science Research Resources Bank (Osaka, Japan). HeLa cells were kindly donated by Dr. Tomohito Kakegawa, Department of Biochemistry, Graduate School of Pharmaceutical Sciences, Chiba University.

Full-length cDNA cloning

Full-length human OATP1B1 (also known as LST-1, OATP2 and OATP-C, *gene SLC21A6/SLCO1B1*) coding sequences corresponding to nucleotides 67-2247 of GeneBank accession No. AF205071 was amplified from human liver cDNA using the primer pair 5'-AATC-CAGGTGATTGTTTCAAACTGAGCATC-3' (forward) and 5'-TGGAAACACAGAAGCAGAAGT-3' (reverse). The polymerase chain reaction (PCR) was performed using KOD-Plus-DNA polymerase (Toyobo, Osaka, Japan) according to the following schedule: 2 min denaturation/activation at 94°C, followed by three cycles with 30 s denaturation at 94°C, 30 s annealing at 66°C, 90 s elongation at 68°C, three cycles with 30 s denaturation at 94°C, 30 s annealing at 63°C, 90 s elongation at 68°C, three cycles with 30 s denaturation at 94°C, 30 s annealing at 60°C, 90 s elongation at 68°C, three cycles with 30 s denaturation at 94°C, 30 s annealing at 57°C, 90 s elongation at 68°C, and, subsequently, 28 cycles with 30 s denaturation at 94°C, 30 s annealing at 54°C, 105 s elongation at 68°C, and a final elongation at 68°C for 3 min. The amplicon was subcloned into pCR-Blunt II-TOPO vector and the sequence was verified as coding *SLCO1B1*1b* using dye terminator sequencing (CEQ2000XL DNA Analysis System, Beckman Coulter, Inc., Fullerton, CA). *SLCO1B1*1b* cDNA, located between *Kpn*I and *Not*I multiple cloning sites, was subcloned into pcDNA3.1/Zeo.

Site-directed mutagenesis

Point mutations were introduced into *SLCO1B1*1b*/pcDNA3.1/Zeo using KOD-Plus DNA polymerase followed by digestion of the template DNA with *Dpn*I. Oligonucleotides containing 388A > G and 521T > C were used to create *SLCO1B1*1a* and *SLCO1B1*15* expression vectors, respectively. 521T > C was also introduced into *SLCO1B1*1a* vector in order to create *SLCO1B1*5* expression vector. Similarly, 1007C > G mutated vectors were constructed from *SLCO1B1*1a*, *SLCO1B1*1b*, *SLCO1B1*5* and *SLCO1B1*15* vectors. The presence of the mutations was verified by full sequencing. Obtained *SLCO1B1* variant vectors are shown in Table 1. Primers used for site-directed mutagenesis were as follows: A388G, 5'-GAAACTAATATCAATTCATCA-GAAAATTC-3' (forward) and 5'-GAATTTTCTGATGA-ATTGATATTAGTTTC-3' (reverse); T521C, 5'-CATG-TGGATATATGCGTTCATGGGTA-3' (forward) and

Table 1 *SLCO1B1* allelic variants prepared by site-directed mutagenesis

	Mutation (amino acid substitution)		
	A388G (Asn130Asp)	T521C (Val174Ala)	C1007G (Pro336Arg)
*1a	A	T	C
*1b	G	T	C
*5	A	C	C
*15	G	C	C
*1a+C1007G^a	A	T	G
*1b+C1007G^a	G	T	G
*5+C1007G^a	A	C	G
*15+C1007G	G	C	G

^aThese alleles have not been reported as naturally occurring variants.

5′-TACCCATGAAC**G**CATATATCCACATG-3′ (reverse); C1007G, 5′-CATCCTTACTAATC**G**CCTGTATGTTA-TG-3′ (forward) and 5′-CATAACATACAGGC**G**GATTAG-TAAGGATG-3′ (reverse). The PCR site-directed mutagenesis was performed under the following conditions: 2 min denaturation/activation at 94°C followed by 12 cycles with 20 s denaturation at 95°C, 30 s annealing at 50°C and 8 min elongation at 68°C.

Cell culture and expression

For transient expression, the transfection of plasmids into HEK293 cells or HeLa cells was performed using Lipofectamine 2000 (Invitrogen) or Lipofectamine Plus (Invitrogen), respectively, according to the manufacturer's protocol. Briefly, HEK293 cells seeded at a density of 2–4 10^5 cells per well in a poly-D-lysine coated 12-well plate were cultured in Dulbecco's modified Eagle's medium (DMEM) supplemented with 10% fetal bovine serum (FBS) and transfected with complexes of 1.5 μg of plasmid and 3 μl of Lipofectamine 2000 reagents diluted in OPTI-MEM I (Invitrogen). HeLa cells seeded at 1–1.2 10^5 cells per well in a 12-well plate were cultured in RPMI-1640 medium supplemented with 10% FBS and penicillin–streptomycin. At 1 day after seeding, the cells were exposed to antibiotics-free DMEM containing serum and then transfected with complexes of 0.5 μg of plasmid, 3 μl of Lipofectamine and 2 μl of Plus reagent in DMEM. At 3 h after the initiation of transfection, the medium was changed to complete RPMI-1640 medium. At 1 day prior to assays, cells were treated with sodium butyrate to enhance the expression of OATP1B1 proteins. HEK293 cells and HeLa cells transfected with the pcDNA3.1 vector alone were used to obtain background activity (termed mock). The expression of OATP1B1 was verified by reverse transcriptase (RT)–PCR.

RT–PCR analysis

Total RNA was extracted by using Trizol reagent (Invitrogen) from transfected cells that had been exposed to sodium butyrate for 1 day. After treatment with DNase I (TaKaRa, Kyoto, Japan), cDNA synthesis was performed by using Ready-To-Go RT-PCR beads (Amersham Biosciences Corp., Piscataway, New Jersey, USA) with oligo d(T)$_{12-18}$ primers and 1 U of RNaseOUT (Invitrogen)

according to the manufacturer's protocol. Then, the PCR reaction was performed using Ex-Taq (TaKaRa) as follows: 2 min denaturing at 94°C, 37 cycles with 15 s denaturing at 94°C, 30 s annealing at 49°C, 40 s elongation at 72°C, and a final elongation for 1 min at 72°C. The specific primer pairs for OATP1B1 designed by Tamai *et al.* [15] and glyceraldehyde-3-phosphate-dehydrogenase (GAPDH) were as follows: OATP1B1, 5′-TGTCATT-GTCCTTTTACCTATTAT-3′ (forward) and 5′-TGTAA-GTTATTCCATTGTTTCCAC-3′ (reverse); GAPDH, 5′-TGCACCACCAACTGCTTA-3′ (forward) and 5′-GG-ATGCAGGGATGATGTTC-3′ (reverse). Products were run with 3% agarose gel. *SLCO1B1***1b*/pcDNA3.1 vector and distilled water were used as templates for positive and negative controls, respectively.

Transport assays

For transport assays, the transfected cells in 12-well plates were treated with sodium butyrate for 1 day. The medium was changed to DMEM free from both antibiotics and serum without a substrate. To assess transport, the medium was removed and the same medium containing a substrate was added. The monolayers were incubated for 1–5 min depending on the substrate, and then cells were rapidly washed once or twice with ice-cold DMEM containing 5% FBS and three times with ice-cold DMEM. For [^{3}H]-labeled substrates, cells were lysed in 500 μl of 0.2% sodium dodecyl sulfate, and 400-μl aliquots were transferred to scintillation vials and 25-μl aliquots of cell lysate were used to determine protein concentrations by the method of Lowry with bovine serum albumin (BSA) as a standard. Radioactivity was measured by a liquid scintillation counter (LSC 6100, Aloka Co., Tokyo, Japan). For un-radiolabeled substrates, 500 μl of ice-cold solution consisting of sodium acetate (pH 4.5; 10 mM)-acetonitrile-methanol (2:1:1, v/v/v) was added, and the solution containing cells was transferred to a centrifuge tube and then the substrate accumulated in cells was extracted by sonication for 10 min at 4°C. After centrifugation at 17 000 g for 10 min at 4°C, a 400-μl aliquot of the supernatant was transferred to Ultrafree-MC (Millipore, Billerica, Massachusetts, USA) and filtered by centrifugation at 5000 g for 5 min at 4°C, and the obtained filtrate was stored at −80°C until

quantitation. To the cell pellet, 400 µl of 0.1 N NaOH was added and solubilized, and then a 25-µl aliquot of cell lysate was used to determine protein concentration by the method of Lowry with BSA as a standard. Transport for estradiol-17β-D-glucuronide and estrone-3-sulfate was determined after 3 and 1 min of incubation, periods within which uptake rate was not saturated, with concentrations of 500 nM and 50 nM at 37°C, respectively. The uptake rate was estimated by subtracting uptake by mock cells from total uptake by SLCO1B1 cDNA-transfected cells and expressed as a percentage of SLCO1B1*1a (reference allele). For transport assay of statins, a preliminary study was carried out to estimate IC50 values of statins by examining the transporting activity for estradiol-17β-D-glucuronide and estrone-3-sulfate substrate in the absence or presence of various concentrations of statins. IC50 values estimated were: approximately 10 µM for atorvastatin and cerivastatin and approximately 100 µM for pravastatin and simvastatin. Thus, the substrate concentrations in the transport medium were set at 20 µM for pravastatin, 0.5 µM for atorvastatin and cerivastatin, and 10 µM for simvastatin so that the substrate concentrations would be lower than those at which half the maximal uptake occurs (K_m). The incubation period for pravastatin was set at 5 min and the incubation periods for atorvastatin, cerivastatin and simvastatin were set at 1 min in order to determine the initial uptake rate. The uptake rate was expressed as cell-to-medium ratio, which was estimated by dividing the amount of statins accumulated in cells by the substrate concentration in the transport medium.

Kinetic analysis

Transport for pravastatin and atorvastatin was determined after 5 and 1 min of incubation with 5, 10, 20, 50 and 100 µM and with 0.5, 2, 5, 20 and 50 µM at 37°C, respectively. The OATP1B1-mediated uptake was calculated after subtracting the uptake by the mock cells from the uptake by SLCO1B1 cDNA-transfected cells at each concentration. Michaelis–Menten-type nonlinear curve fitting was carried out to obtain kinetic parameters of the maximal uptake rate (V_{max}) and K_m (DeltaGraph 4.5, RockWare Inc., Golden, Colorado, USA).

Analytical procedures for 3-hydroxy-3-methylglutaryl coenzyme A reductase inhibitors (statins)

Quantitation of statins was performed using HPLC tandem mass spectrometry. The HPLC system consisted of three LC-10ADVP pumps, a SLC-10AVP controller, a SIL-HTC auto-injector and a FCV-12AH switching valve (Shimadzu, Kyoto, Japan). The HPLC column used was a CAPCELL PAK C8 UG120 (5 µm in particle size, 4.6 × 35 mm, Shiseido, Tokyo, Japan). Aliquots (pravastatin, 100 µl; atorvastatin, cerivastatin, simvastatin, 10 µl) of samples were injected onto the column with the mobile phase consisting of methylammonium acetate (pH 4.5; 1 mM)-acetonitrile-methanol (70:15:15; v/v/v; eluate C) at

a flow rate of 1.2 ml/min. After 1 min, the mobile phase was changed to a mixture of methylammonium acetate (pH 4.5; 1 mM)-acetonitrile-methanol (30:35:35; v/v/v; eluate A) and methylammonium acetate (pH 4.5; 1 mM)-acetonitrile-methanol (10:45:45; v/v/v; eluate B) at a flow rate of 0.5 ml/min using a gradient program described below, and the eluate was taken into the mass spectrometer. After 5 min, the solvent was switched to eluate C to re-equilibrate the column. The time program of the mixture ratio of eluate A and eluate B was set as follows: 0% B for 0–1.2 min, linear gradient from 0 to 100% B for 1.2–3.5 min, 100% B for 3.5–4.7 min, linear gradient from 100 to 0% B for 4.7–4.8 min, and then 0% B for 4.8–7.0 min. The analytes were detected by an API4000 tandem mass spectrometer with a turbo-ion spray interface (Applied Biosystems, Foster, California, USA). All analytes were detected in positive mode, and the precursor to product ions monitored were m/z 447.3 > m/z 327.3 (pravastatin), m/z 559.3 > m/z 440.4 (atorvastatin), m/z 460.3 > m/z 356.1 (cerivastatin), and m/z 441.3 > m/z 325.3 (simvastatin). Samples for calibration, validation and quality control were prepared in a manner similar to that used for preparation of analytical samples described above. Briefly, untransfected HEK293 cells seeded on a 12-well plate were washed three times with ice-cold DMEM, and extraction solution spiked with known amounts of standards was added. Then the following procedures (i.e. extraction and filtration) were carried out. The quantitative range of analytes was determined by intra-day reproducibility assays in which the limit of quantitation was set at 0.25 nM for pravastatin, atorvastatin and cerivastatin and at 2.5 nM for simvastatin, as these were sufficient to estimate the lowest concentrations at which acceptable accuracy ($< 100 \pm 20\%$) and imprecision ($< \pm 20\%$) were obtained.

Immunofluorescence microscopy

Transfected cells were grown on chamber slides (Nalge Nunc International, Naperville, Illinois, USA). Sodium butyrate was added to the culture medium 1 day before the experiment. After washing twice with PBS, the monolayers were fixed with 4% formaldehyde in PBS. After rinsing cells with PBS, the cells were incubated with 0.05% Tween 20 in PBS (PBS-T) containing 3% BSA for 30 min at room temperature for blocking. The monolayers were incubated with the previously described primary antibody against OATP1B1 (1:50-fold in PBS-T) for 1 h at room temperature. Cells were washed four times with PBS-T and then incubated with PBS-T containing goat anti-rabbit IgG labeled with Alexa Fluor 488 (Molecular Probes, Inc., Eugene, Oregon, USA) for 1 h at room temperature. After washing cells twice with PBS-T, about two drops of ProLong Antifade reagent/mounting mixture (Molecular Probes) were added to the slide. Confocal laser-scanning immunofluorescence microscopy was performed using FluorView FV-500 (Olympus, Tokyo, Japan).

Results

Expression of SLCO1B1 in HEK293 and HeLa cells

Levels of OATP1B1 mRNA transiently expressed in HEK293 and HeLa cells were analyzed by RT–PCR. As shown in Fig. 1, the levels of mRNA were apparently equal among OATP1B1*1a and variants in either of HEK293 or HeLa cells.

Transport activity of SLCO1B1 allelic variants for typical substrates

The relative transporting activities of the SLCO1B1 variants for estradiol-17β-D-glucuronide and estrone-3-sulfate are shown in Fig. 2. The transporting activities for these typical substrates of OATP1B1 significantly decreased in either HEK293 and HeLa cells expressing SLCO1B1*5, *15, *5 + C1007G and *15 + C1007G. The extents of decrease were not greatly different among these variants, ranging from −37% to −73% of that of SLCO1B1*1a. In contrast, there was no apparent tendency of changes in the activities of cells expressing SLCO1B1*1b, *1a + C1007G and *1b + C1007G, which ranged from 85% to 130% of that of SLCO1B1*1a.

Transport activity of OATP1B1 allelic variants for statins

Since the effects of OATP1B1 variants on activities for the uptake of typical substrates of OATP1B1 were similar
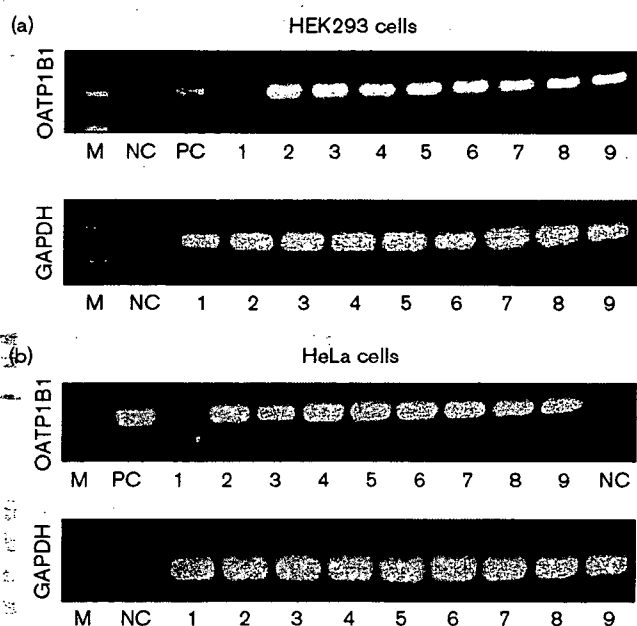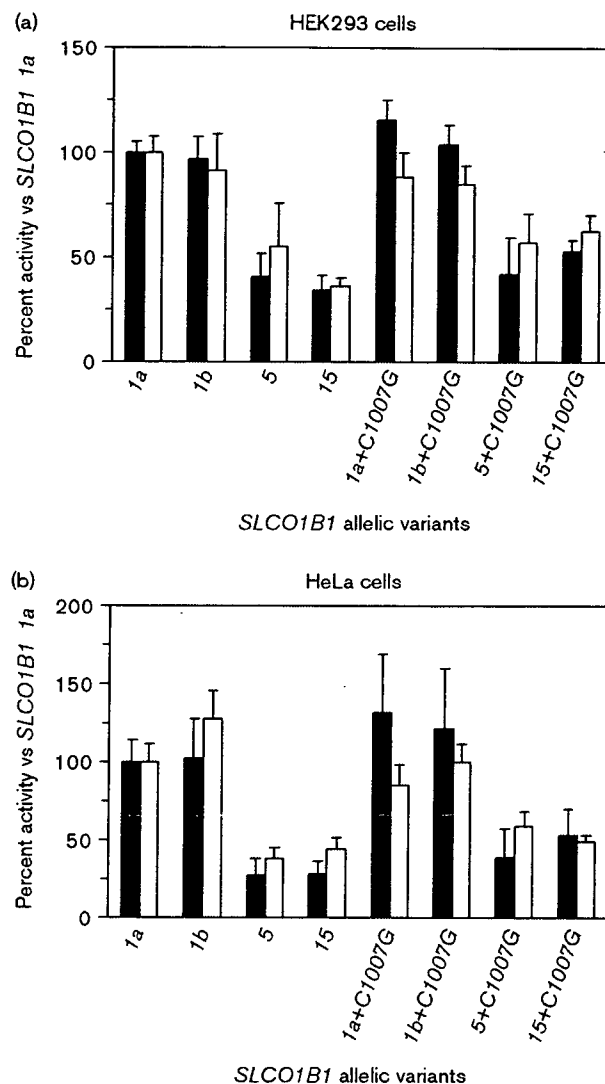
Fig. 1

(a) HEK293 cells

(b) HeLa cells

RT–PCR analysis of mRNA expression of (a) OATP1B1 and GAPDH in HEK293 cells and (b) OATP1B1 and GAPDH in HeLa cells transiently expressing SLCO1B1 allelic variants. Specific bands corresponding to OATP1B1 and GAPDH are shown with sizes of 194 and 177 base pairs, respectively. M, marker; NC, negative control; PC, positive control; 1, mock; 2, OATP1B1*1a; 3, OATP1B1*1b; 4, OATP1B1*5; 5, OATP1B1*15; 6, OATP1B1*1a + C1007G; 7, OATP1B1*1b + C1007G; 8, OATP1B1*5 + C1007G; 9, OATP1B1*15 + C1007G.

Fig. 2

(a) HEK293 cells

SLCO1B1 allelic variants

(b) HeLa cells

SLCO1B1 allelic variants

Uptake of [³H]estradiol-17β-glucuronide (closed bars) and [³H]estrone-3-sulfate (open bars) into (a) HEK293 cells and (b) HeLa cells transiently expressing SLCO1B1 allelic variants. Each bar represents the mean and S.D. of three independent assays. $*P < 0.05$, $**P < 0.01$, $***P < 0.001$ significantly different from the uptake by SLCO1B1*1a.

in HEK293 and HeLa cells, the effects of these valiant alleles on the transport of statins were studied using only HEK293 cells. Similar to the results for typical substrates of OATP1B1, transporting activities for pravastatin, atorvastatin and cerivastatin decreased significantly in HEK293 cells expressing SLCO1B1*5, *15, *5 + C1007G and *15 + C1007G, whereas those of SLCO1B1*1b, *1a + C1007G and *1b + C1007G were not apparently different from that of SLCO1B1*1a (Fig. 3a–c). However, the extents of decreases in the activities of cells expressing SLCO1B1*5, *15, *5 + C1007G and *15 + C1007G appeared to be different among statins when they were compared with the activity of SLCO1B1*1a.

Fig. 3
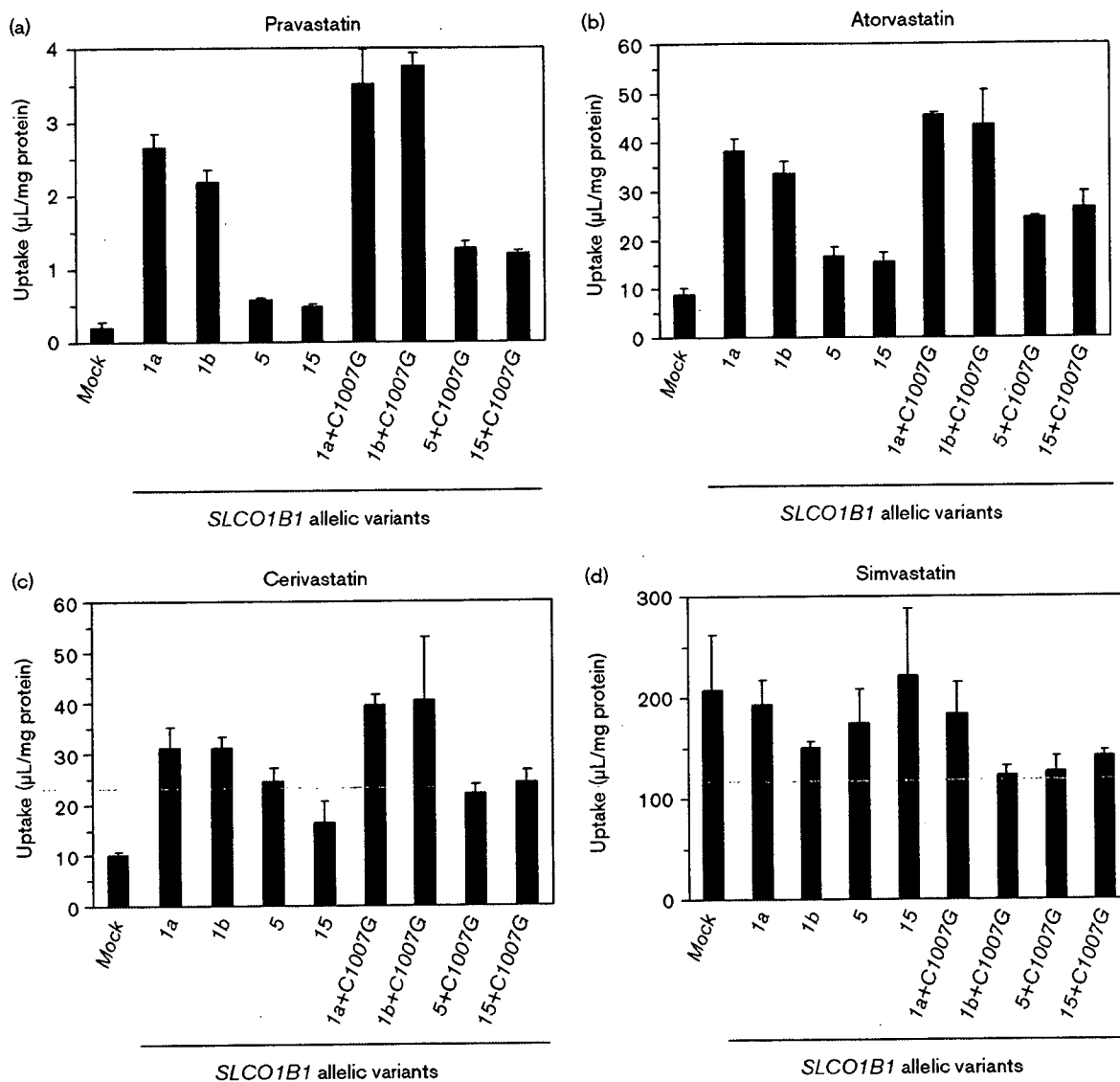
Uptake of statins into HEK293 cells transiently expressing SLCO1B1 allelic variants. (a) pravastatin, (b) atorvastatin, (c) cerivastatin, and (d) simvastatin. Each bar represents the mean and S.D. of triplicated determinations.

The most prominent decrease was found for pravastatin followed by atorvastatin and cerivastatin. In contrast, a tendency of decreases such as that found in the typical substrates and the three statins was not observed for simvastatin, for which the activities of cells expressing SLCO1B1*5 and *15 were not different from that of SLCO1B1*1a and those of SLCO1B1*1a and its variants were comparable or less than that of mock (Fig. 3d).

Kinetic analysis

Since the effects of SLCO1B1*5, *15 and *15 + C1007G on the transporting activity of OATP1B1 for statins were most prominent for pravastatin and atorvastatin, the effects of SLCO1B1*1b, *5, *15 and *15 + C1007G on the kinetics of these statins were studied using HEK293 cells. As shown in Fig. 4, saturable transport was observed for both statins. The kinetic parameters estimated are summarized in Table 2. Although the differences were not so apparent for K_m values of these statins among the five haplotypes studied, the V_{max} values of cells expressing SLCO1B1*5, *15 and *15 + C1007G were significantly lower than that of SLCO1B1*1a. Accordingly, intrinsic clearance (V_{max}/K_m) of pravastatin and atorvastatin decreased by 79%, 80% and 61% and by 67%, 60% and 66% for SLCO1B1*5, *15 and *15 + C1007G, respectively, as compared to SLCO1B1*1a.

Table 2 Kinetic parameters of pravastatin and atorvastatin uptake by SLCO1B1 allelic variants

Substrate	SLCO1B1 allelic variants	N	K_m(μM)	V_{max}(pmol/min/mg)	V_{max}/K_m(μl/min/mg)
Pravastatin					
	*1a	5	85.7±29.8	58.2±4.1	0.753±0.291
	*1b	5	88.7±20.6	61.0±19.0	0.722±0.263
	*5	5	153±80	22.4±9.0***	0.155±0.022*
	*15	4	118±69	17.0±8.1***	0.154±0.030*
	*15+C1007G	5	145±38*	40.8±5.2***	0.294±0.073*
Atorvastatin					
	*1a	4	12.4±4.8	70.4±29.9	5.65±0.95
	*1b	4	12.7±4.5	59.3±10.5	5.01±1.22
	*5	3	11.1±7.6	16.0±4.3*	1.88±1.16**
	*15	3	9.29±2.83	19.2±2.4*	2.28±1.08**
	*15+C1007G	3	13.1±6.1	23.3±7.4*	1.91±0.59**

N means numbers of assays;
*$P<0.05$,
**$P<0.01$,
***$P<0.001$ significantly different from the uptake by SLCO1B1*1a.

Cell surface expression of OATP1B1 allelic variants

Since SLCO1B1 allelic variants did not alter either the mRNA levels or K_m values of statins, the decrease in intrinsic clearance could be derived from the reduced level of functional OATP1B1 protein in the plasma membrane. Accordingly, immunocytochemical analysis was performed to examine the cellular localization of OATP1B1 variants. Fig. 5 shows the staining of OATP1B1 proteins in HEK293 cells transfected with SLCO1B1*1a, *1b, *5, *15, *15+C1007G and mock vectors. SLCO1B1*1a and *1b allelic proteins were mainly localized at the plasma membrane, whereas SLCO1B1*5, *15 and *15+C1007G allelic proteins were observed both in the intracellular space and at the plasma membrane. Similar results were also obtained for HeLa cells transfected with vectors of these SLCO1B1 allelic variants (data not shown).

Discussion

The results of the present study clearly showed that the transporting activities of OATP1B1 for its typical substrates, estradiol-17β-D-glucuronide and estrone-3-sulfate, and for three statins, pravastatin, atorvastatin and cerivastatin, decreased significantly in HEK293 and/or HeLa cells expressing SLCO1B1*5, *15, *5+C1007G and *15+C1007G, whereas those of SLCO1B1*1b, *1a+C1007G and *1b+C1007G were not apparently different from those of SLCO1B1*1a (Figs 2, 3 and 4). Since SLCO1B1*5 contains 521T > C and SLCO1B1*15 contains both of 388A > G and 521T > C, the results suggest that 521T > C is the key SNP for determining the functional alteration of OATP1B1. This contention is in good agreement with the present findings that SLCO1B1*5, *15 and *15+C1007G allelic proteins are localized not only at the plasma membrane but also in the intracellular space in both HeLa cells and HEK293 cells, suggesting that decreased activities of cells expressing SLCO1B1*5, *15 and *15+C1007G are mainly and commonly derived from a sorting error caused by

521T > C that substitutes a valine to an alanine residue at position 174 in OATP1B1, which is putatively located on transmembrane-spanning domain 4 [8].

The present in-vitro findings are consistent with previous in-vivo observations that the area under the plasma concentration–time curve (AUC) of pravastatin was significantly greater in carriers of the haplotype of SLCO1B1*5 or *15 than that of SLCO1B1*1a or *1b [12,14,16]. However, the extent of decrease in the transporting capacity of OATP1B1 by the mutation of SLCO1B1*5 and *15 in vivo is difficult to assess because information on non-renal clearance of pravastatin in homozygote of SLCO1B1*5 or *15 is limited. However, the value of pravastatin reported in one subject who is homozygous for SLCO1B1*15 was 86 to 87% lower and those in heterozygotes of SLCO1B1*15 were 45 to 50% lower than those in homozygotes of SLCO1B1*1a or *1b [14]. These values are in good agreement with or explainable by the results of the present study showing that V_{max}/K_m of pravastatin uptake in HEK293 cells expressing SLCO1B1*15 was 80% and 79% lower than those of SLCO1B1*1a and *1b, respectively (Table 2).

Contradicting results have been reported for the influence of SLCO1B1*5 on the function of OATP1B1 in cDNA-expression systems in which transporting activities of cells expressing SLCO1B1*5 for estradiol-17β-D-glucuronide and estrone-3-sulfate were reduced to less than half of those of SLCO1B1*1a when they were transiently expressed in HeLa cells [8], whereas the activities for estrone-3-sulfate were not different between SLCO1B1*5 and *1a in HEK293 cells [13]. The results of the present study showed that transporting activities of SLCO1B1*5 allelic protein decreased to less than or around 50% of those of SLCO1B1*1a for both 17β-D-glucuronide and estrone-3-sulfate in HeLa cells and even in HEK293 cells, being consistent with results reported by Tirona et al. [8]. Therefore, the capacity of

119

Fig. 4

(a)

(b)
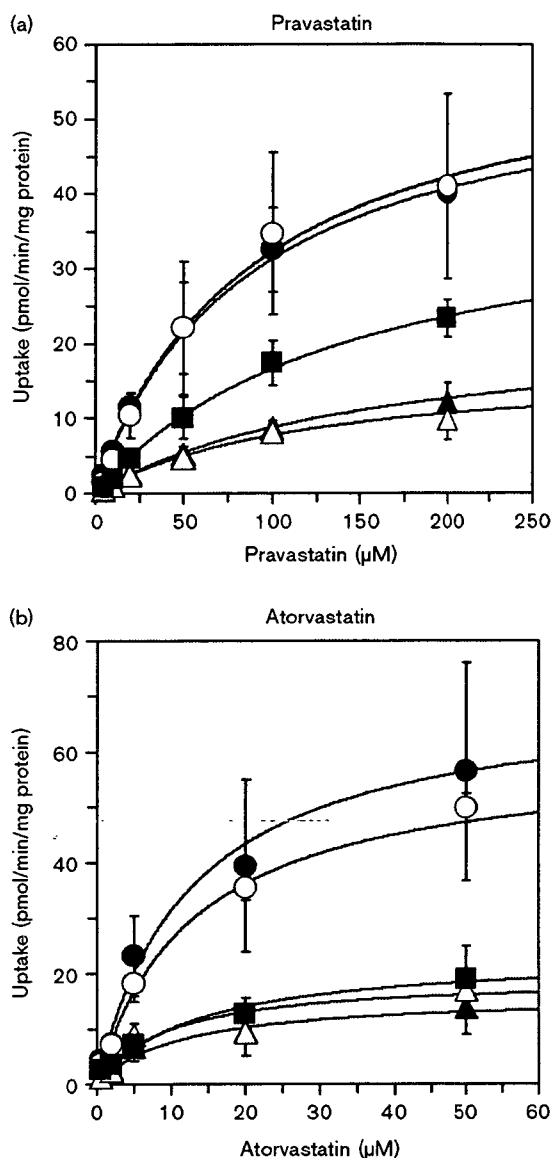
Concentration dependence of (a) pravastatin and (b) atorvastatin uptake into HEK293 cells transiently expressing SLCO1B1*1a (closed circles), *1b (open circles), *5 (closed triangles), *15 (open triangles) or *15 + C1007G (closed squares). Each value is the mean ± SD of at least three independent assays, and the solid lines represent the results of nonlinear least-squares analysis.

*SLCO1B1*5* allelic protein is considered to be decreased both *in vitro* [8] and *in vivo* [12,14,16], although it remains unknown why there were contradicting findings in previous studies. It is possible that such characteristics were altered by maintenance conditions such as additional chemicals used for transfection or sodium butyrate.

The results of the present study showed that 388A > G did not alter the activity of OATP1B1 significantly. This contradicts the finding reported by Mwinyi *et al.* [12] that

Fig. 5
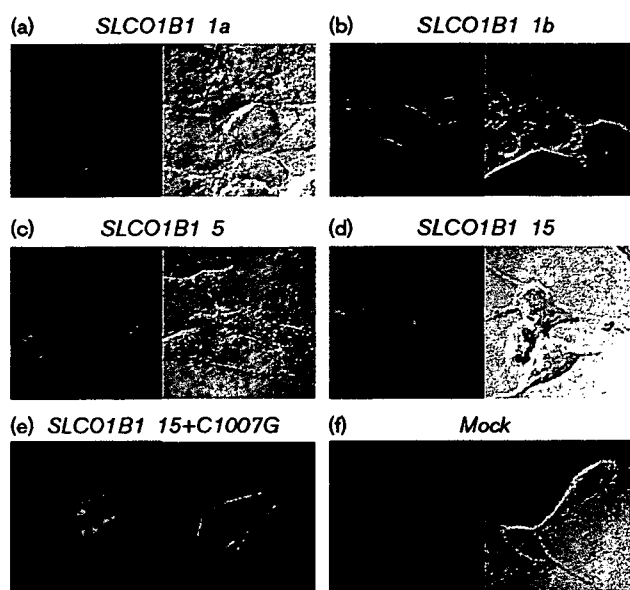
Immunolocalization of (a) SLCO1B1*1a, (b) SLCO1B1*1b, (c) SLCO1B1*5, (d) SLCO1B1*15, (e) SLCO1B1*15 + C1007G allelic proteins, and (f) mock in HEK293 cells. Fluorescent images are shown on the left, and phase contrast images are shown on the right.

the AUC of pravastatin was 60% smaller in subjects carrying *SLCO1B1*1b* than that in homozygous subjects of *1a*, suggesting that uptake of pravastatin by OATP1B1 is increased by 388A > G. Nonetheless, our findings are consistent with results of three independent in-vitro studies [8,13,17] and one in-vivo study showing that *1b* does not affect the activity of OATP1B1 [14]. Therefore, it is conceivable that 388A > G does not alter the transporting activity of OATP1B1 at least when pravastatin is used as a substrate, although further in-vivo study is needed to confirm our and others' in-vitro findings [8,13,17]. The present results also suggest that 1007C > G does not influence the activity of OATP1B1 dramatically, although it substitutes a proline to an arginine residue at position 336 in OATP1B1 that is putatively located on transmembrane-spanning domain 7. It is notable that 1007C > G is the first example of a nonsynonymous SNP that does not appear to affect the function of OATP1B1 despite its localization on a transmembrane-spanning domain. All of the mutations localized on the putative transmembrane-spanning domain of OATP1B1 reported previously are associated with significant reduction in their transporting activities [8].

Of the four statins studied, the most prominent decrease in the activities of cells expressing *SLCO1B1*5* or *15* was found for pravastatin followed by atorvastatin and cerivastatin, but no apparent decrease was found for simvastatin when the activities were compared with

*SLCO1B1*1a* (Fig. 3). This tendency may be explained by the physicochemical properties of statins. The water/octanol partition coefficients of pravastatin, atorvastatin, cerivastatin and simvastatin have been reported to be −0.47, 1.53, 2.32 and 4.40, respectively [18], which are in the same order as that of less decreases in the activities for statins. This phenomenon appears to be derived from the extent to which OATP1B1 contributes to the total transmembrane distribution of statins that includes passive diffusion. Comparing the uptake rates in mock among these statins, which would express the sum of passive diffusion and active transport in a background, the uptake rate of simvastatin was about 20-fold higher than that of atorvastatin and cerivastatin and about 2000-fold higher than that of pravastatin. These findings indicate that the transporting activity of OATP1B1 for simvastatin is much less than the passive diffusion because of its high lipophilicity. On the other hand, atorvastatin and cerivastatin are transported in part by passive diffusion because of their moderate lipophilicity, while pravastatin is not transported extensively by passive diffusion because of its hydrophilicity. Thus, it is thought that the uptake of pravastatin is affected remarkably and the uptake of atorvastatin and cerivastatin is affected moderately by mutations carrying 521T > C. However, further in-vivo studies are clearly needed to confirm these contentions because these findings were derived from an in-vitro study and may not reflect the activity of OATP1B1 *in vivo*.

The present study showed that the uptake clearances (V_{max}/K_m) of atorvastatin and pravastatin decreased to 20 to 40% of cells expressing *SLCO1B1*1a* and that the uptake of cerivastatin at a fixed concentration also decreased to 31 to 69% of *SLCO1B1*1a* in the variants of *SLCO1B1* carrying 521T > C. Since the allele frequencies of *SLCO1B1*5* have been reported to be 14%, 2% and 0.7% in European-American, African-American and Japanese, respectively [8,13] and those of *SLCO1B1*15* have been reported to be 10 to 15% in Japanese [13,14], homozygous of T521C is estimated to exist in at least one of 40 to 50 of European-Americans and Japanese. These findings suggest that 521T > C is a major factor influencing the disposition and even efficacy or adverse reactions of drugs transported by OATP1B1. For example, it is possible that *SLCO1B1*5* and *15* may be one of the risk factors attaining adverse drug reactions such as myopathy or rhabdomyolysis due to statins which has been reported to be dependent on the plasma concentration of statins [19]. In this regard, the possibility that an acid form of simvastatin that is an active form of simvastatin could be transported by OATP1B1 should be noted, although the results of the present study suggest that simvastatin (lactone form) is not efficiently taken up by OATP1B1. Further study is needed to clarify the effect of polymorphisms on transporting activity of OATP1B1 for the acid form of simvastatin. In addition, contribution of other transporters such as OATP1B3 and OATP2B1 should be considered to estimate the effect of SNPs in the *SLCO1B1* on hepatic clearance of drugs *in vivo*.

In conclusion, the results of current study suggest that T521C is the key SNP that causes a sorting error of OATP1B1 and decreases the functional activity of variant proteins derived from *SLCO1B1*5, *15* and *15 + C1007G*.

References

1 Kusuhara H, Sugiyama Y. Role of transporters in the tissue-selective distribution and elimination of drugs: transporters in the liver, small intestine, brain and kidney. *J Control Rel* 2002; 78:43–54.

2 Abe T, Kakyo M, Tokui T, Nakagomi R, Nishio T, Nakai D, et al. Identification of a novel gene family encoding human liver-specific organic anion transporter LST-1. *J Biol Chem* 1999; 274:17159–17163.

3 Hsiang B, Zhu Y, Wang Z, Wu Y, Sasseville V, Yang WP, et al. A novel human hepatic organic anion transporting polypeptide (OATP2). *J Biol Chem* 1999; 274:37161–37168.

4 Tirona RG, Kim RB. Pharmacogenomics of organic anion-transporting polypeptides (OATP). *Adv Drug Deliv Rev* 2002; 54:1343–1352.

5 Tamai I, Nezu J, Uchino H, Sai Y, Oku A, Shimane M, et al. Molecular identification and characterization of novel members of the human organic anion transporter (OATP) family. *Biochem Biophys Res Commun* 2000; 273:251–260.

6 Cui Y, Konig J, Leier I, Buchholz U, Keppler D. Hepatic uptake of bilirubin and its conjugates by the human organic anion transporter SLC21A6. *J Biol Chem* 2001; 276:9626–9630.

7 Kullak-Ublick GA, Ismair MG, Stieger B, Landmann L, Huber R, Pizzagalli F, et al. Organic anion-transporting polypeptide B (OATP-B) and its functional comparison with three other OATPs of human liver. *Gastroenterology* 2001; 120:525–533.

8 Tirona RG, Leake BF, Merino G, Kim RB. Polymorphisms in OATP-C: identification of multiple allelic variants associated with altered transporting activity among European- and African-Americans. *J Biol Chem* 2001; 276:35669–35675.

9 Tirona RG, Leake BF, Wolkoff AW, Kim RB. Human organic anion transporting polypeptide-C (SLC21A6) is a major determinant of rifampicin-mediated pregnane X receptor activation. *J Pharmacol Exp Ther* 2003; 304:223–228.

10 Shitara Y, Itoh T, Sato H, Li AP, Sugiyama Y. Inhibition of transporter-mediated hepatic uptake as a mechanism for drug–drug interaction between cerivastatin and cyclosporin A. *J Pharmacol Exp Ther* 2003; 304:610–616.

11 Schneck DW, Birmingham BK, Zalikowski JA, Mitchell PD, Wang Y, Martin PD, et al. The effect of gemfibrozil on the pharmacokinetics of rosuvastatin. *Clin Pharmacol Ther* 2004; 75:455–463.

12 Mwinyi J, Johne A, Bauer S, Roots I, Gerloff T. Evidence for inverse effects of OATP-C (SLC21A6) 5 and 1b haplotypes on pravastatin kinetics. *Clin Pharmacol Ther* 2004; 75:415–421.

13 Nozawa T, Nakajima M, Tamai I, Noda K, Nezu J, Sai Y, et al. Genetic polymorphisms of human organic anion transporters OATP-C (SLC21A6) and OATP-B (SLC21A9): allele frequencies in the Japanese population and functional analysis. *J Pharmacol Exp Ther* 2002; 302:804–813.

14 Nishizato Y, Ieiri I, Suzuki H, Kimura M, Kawabata K, Hirota T, et al. Polymorphisms of OATP-C (SLC21A6) and OAT3 (SLC22A8) genes: consequences for pravastatin pharmacokinetics. Clin Pharmacol Ther 2003; 73:554–565.

15 Tamai I, Nozawa T, Koshida M, Nezu J, Sai Y, Tsuji A. Functional characterization of human organic anion transporting polypeptide B (OATP-B) in comparison with liver-specific OATP-C. Pharm Res 2001; 18: 1262–1269.

16 Niemi M, Schaeffeler E, Lang T, Fromm MF, Neuvonen M, Kyrklund C, et al. High plasma pravastatin concentrations are associated with single nucleotide polymorphisms and haplotypes of organic anion transporting polypeptide-C (OATP-C, SLCO1B1). Pharmacogenetics 2004; 14: 429–440.

17 Michalski C, Cui Y, Nies AT, Nuessler AK, Neuhaus P, Zanger UM, et al. A naturally occurring mutation in the SLC21A6 gene causing impaired membrane localization of the hepatocyte uptake transporter. J Biol Chem 2002; 277:43058–43063.

18 Matsuyama K, Nakagawa K, Nakai A, Konishi Y, Nishikata M, Tanaka H, et al. T. Evaluation of myopathy risk for HMG-CoA reductase inhibitors by urethane infusion method. Biol Pharm Bull 2002; 25:346–350.

19 Thompson PD, Clarkson P, Karas RH. Statin-associated myopathy. JAMA 2003; 289:1681–1690.

In Vivo Metabolic Activity of CYP2C19 and CYP3A in Relation to CYP2C19 Genetic Polymorphism in Chronic Liver Disease

Akihiro Ohnishi, MD, PhD, Shigeto Murakami, MD, PhD, Setsuko Akizuki, PhD, Junko Mochizuki, MD, Hirotoshi Echizen, MD, PhD, and Ichiro Takagi, MD, PhD

To study whether chronic liver disease (CLD) and genetic polymorphism affect the hepatic activity of cytochrome P450 (CYP) isoforms, we compared in vivo CYP2C19 and CYP3A activities using 3-hour omeprazole hydroxylation index (plasma concentration ratio of omeprazole to its 5-hydroxylated metabolite; a higher index indicates lower CYP2C19 activity) and partial formation clearance of cortisol to 6-hydroxycortisol ($CL_{cortisol\ 6\ -HC}$) in 31 CLD patients (9 with chronic hepatitis; 22 with cirrhosis comprising 20 Child-Pugh type A, 1 type B, and 1 type C) and 30 healthy subjects with different CYP2C19 genotypes. The mean ($\pm$SEM) omeprazole hydroxylation index in CLD patients with homozygous extensive metabolizer (EM) genotype (*1/*1, n = 8), heterozyous EM (*1/*2, n = 11; *1/*3, n = 6) genotypes and poor metabolizer (PM) genotypes (*2/*2, n = 3; *3/*3, n = 3) were 17.15 ± 2.12, 20.02 ± 2.63, and 26.04 ± 3.15, respectively, which were significantly higher compared with control subjects with the corresponding CYP2C19 genotypes (0.81 ± 0.09, 1.55 ± 0.20, and 15.5 ± 1.52). CLD patients with PM genotype

had significantly (P < .05) higher omeprazole hydroxylation indexes than did those with homozygous EM genotype, and those with heterozygous EM genotypes had intermediate values. The mean $CL_{cortisol\ 6\ -HC}$ decreased significantly (P < .001) in CLD patients compared with control subjects (1.19 ± 0.12 versus 2.26 ± 0.24 mL/min). Multiple regression analysis showed that CLD, serum albumin level, and CYP2C19 genotype correlated significantly (P < .05) with the omeprazole hydroxylation index, whereas no significant correlation was observed between $CL_{cortisol\ 6\ -HC}$ and other variables, except CLD. Because CLD and genetic polymorphism of CYP2C19 act additively to reduce CYP2C19 activity, genotyping these patients may be of value in averting adverse reactions of drugs that depend on CYP2C19 for elimination.

Keywords: Chronic liver disease; cirrhosis; cytochrome P450; CYP2C19; CYP3A

Journal of Clinical Pharmacology, 2005;45:1221-1229
©2005 the American College of Clinical Pharmacology

Chronic liver disease (CLD) including cirrhosis, irrespective of the cause, is associated with a reduced number of functional hepatocytes and the development of a pathological intrahepatic portosystemic shunt. As a result, the systemic clearance of drugs that

undergo hepatic metabolism is often reduced in patients with CLD. Drug clearance *via* oxidative drug metabolism (mainly cytochrome P450 [CYP]) is known to be reduced in CLD.[1] Two studies have demonstrated the *in vivo* metabolic activities of 3 major CYP isoforms in patients with mild to moderate CLD,[2,3] using mephenytoin, dapsone, and debrisoquin as the model substrates for CYP2C19, CYP3A4, and CYP2D6, respectively. These studies reported a preferential reduction of CYP2C19 in CLD patients (77% from the healthy controls) compared with CYP3A4 (28%) and CYP2D6 (4%). Several other studies have also examined the differential effect of liver disease on CYP activity.[4-7] Although the existence of such effects of CLD is clinically important in the prescription of drugs in

Table I Demographic and Clinical Characteristic of the Healthy Subjects and Patients With Chronic
Liver Disease Enrolled in the Present Study

	Patients With Chronic Hepatitis	Patients With Cirrhosis	Healthy Controls
No. of subjects or patients	9	22	30
Gender, male/female	8/1	14/8	18/12
Age, y	66 ± 9.5*	70.8 ± 6.1*	50.6 ± 16.4
Child-Pugh score[a]	—	20/1/1	NA
AST, IU/L	47.5 ± 36.8*	78.5 ± 27.1*	25.7 ± 14.1
ALT, IU/L	58.4 ± 65.5*	61.4 ± 23.0*	26.9 ± 8.0
Total protein, g/dL	7.9 ± 0.6	7.4 ± 0.7	7.5 ± 0.5
Albumin, g/dL	4.3 ± 0.5	3.7 ± 0.5*	4.4 ± 0.4
Total bilirubin, mg/dL	0.5 ± 0.2	1.6 ± 3.3	0.6 ± 0.3
Prothrombin index, %	92.6 ± 9.1	77.8 ± 11.5**	ND
Creatinine, mg/dL	0.7 ± 0.22	0.9 ± 0.31	0.8 ± 0.24

Data are mean ± SD; all laboratory data shown are assayed in serum; NA = not applicable; AST = asparate aminotransferase; ALT = alanine aminotransferase; ND = not determined.
a. Classification reported by Pugh et al.[14]
*$P < .05$ compared with control.
**$P < .05$ compared with chronic hepatitis; gender difference was not significant among 3 groups by [2] analysis.

these patients, no subsequent studies have confirmed this finding.

Besides CLD, genetic polymorphism is another important covariate of CYP activity in certain isoforms.[8] Because CYP2C19 is involved in the hepatic metabolism of many therapeutically important drugs, its metabolic activity is under control of genetic polymorphism. At present, as many as 15 variant isoforms have been reported and some of them (eg, CYP2C19*2 and CYP2C19*3 alleles) have been shown to be associated with defective enzyme function.[9] Previous studies[10,11] have shown that the possession of either the CYP2C19*2 or the CYP2C19*3 allele is associated with reduced in vivo CYP2C19 activity, depending on the gene dose; the CYP2C19 activity is lowest in the poor metabolizer (PM) genotypes (CYP2C19*2/*2, *2/*3, or *3/*3), followed by the heterozygous EM genotypes (CYP2C19*1/*2 or *1/*3) and then the homozygous EM genotype (CYP2C19*1/*1). Because the prevalence of defective alleles (CYP2C19*2 and *3) in Asians, including Japanese, is greater than that in whites,[9,12,13] it is importance to study whether the genetic polymorphism of CYP2C19 would have an additive effect on the in vivo CYP2C19 activity, particularly in Japanese patients with CLD.

In this context, the aims of the present study were as follows: (1) to investigate the in vivo CYP2C19 activity in Japanese CLD patients with different CYP2C19 genotypes to assess the degree of interaction between CLD and genetic polymorphism on CYP2C19 activity, (2) to investigate which routine biochemical markers

are clinically useful to predict CYP2C19 activity in CLD patients, and (3) to investigate the CLD-induced changes in CYP3A activity using the 3-hour partial formation clearance of cortisol to 6 -hydroxycortisol (6 -HC) as an in vivo CYP3A index.

MATERIALS AND METHODS

Thirty-one hepatitis C virus (HCV)–positive patients with chronic hepatitis or cirrhosis were studied. The diagnoses were established by histologic findings of liver biopsy and diagnostic imaging using computed tomography and ultrasonography. Table I shows the demographic and clinical characteristics of the 31 patients and the 30 healthy subjects who were enrolled in this study. The study protocol was approved by the Jikei University Ethics Committee. The nature and purpose of the study were fully explained to each subject before written informed consent was obtained.

Nine patients with chronic hepatitis (8 men and 1 woman) aged 52 to 84 years (mean ± SD, 66.0±9.5 years) and weighing 40 to 74 kg (56.9 ± 10.2 kg), as well as 22 biopsy-proven cirrhotic patients (14 men and 8 women) aged 62 to 86 years (70.8±6.1 years) and weighing 38 to 74 kg (55.1±9.0 kg) were studied. The subjects were hospitalized at the Daisan Hospital of Jikei University School of Medicine. All patients were diagnosed as having chronic HCV infection by the detection of HCV-specific messenger RNA and antibody. One cirrhotic patient manifested ascites confirmed by abdominal ultrasonography and computed tomogra-

124

phy. Five cirrhotic patients had endoscopy-confirmed esophageal varices. The severity of liver impairment (cirrhosis) was classified according to the Child-Pugh classification.[14] Among the cirrhotic patients, 20 were graded as type A, 1 as type B, and 1 as type C. None had hepatic encephalopathy or had been treated with a transjugular intrahepatic portosystemic shunt[15] Their clinical and biochemical data are summarized in Table I. They were normotensive and had no abnormalities in 12-lead electrocardiogram (ECG) recordings. All patients had been hospitalized for at least 2 weeks before the study and had no drugs or foods that might have inhibited or induced CYP activity.

Thirty healthy men, aged 25 to 67 years (50.6 ± 16.4 years) and weighing between 32 and 86 kg (61.5 ± 12.7 kg), participated in the study. All subjects were confirmed to be in good general health based on a complete physical examination, a standard 12-lead ECG, hemogram, and clinical laboratory tests. They had no known histories of allergic reactions to drugs or gastrointestinal, renal, hepatic, pulmonary, cardiac, or hematologic disease; they took no drugs or foods that might have an influence on CYP activity.

After fasting overnight, healthy subjects and patients with CLD received 20 mg omeprazole with 200 mL of water, and blood samples were withdrawn at 1.5 hours after dosing to determine plasma cortisol concentration and at 3 hours after dosing to determine plasma concentrations of omeprazole and 5-hydroxy-omeprazole. In addition, 3-hour timed urine samples were collected. DNA samples were extracted from the buffy coat of blood samples, according to the standard protocol described below. All samples were numbered and handled anonymously to ensure the participants' privacy. All enrolled subjects and patients were asked to refrain from smoking during the entire study period.

Genotyping

Seven milliliters of peripheral blood was obtained, and DNA was extracted from peripheral leukocytes using a DNA extraction kit (IsoQuick, Micro Probe Co, Garden Grove, Calif). Genotyping analysis of the polymorphic CYP2C19 genes was performed according to the methods of de Morais et al[12] and Kubota et al.[13] The CYP2C19*2 and CYP2C19*3 alleles were detected by polymerase chain reaction methods using the following allele-specific primers: for identifying the CYP2C19*2 allele, the forward primer was 5 - AATTACAACCAGAGCTTGGC-3 and the reverse primer 5 -TATCACTTTCCATAAAAGCAAG-3 ; for identifying the CYP2C19*3 allele, the forward primer was 5 -AACATCAGGATTGTAAGCAC-3 , and the re-

verse primer was 5 -TCAGGGCTTGGTCAATATAG-3 . Amplified fragments were digested with endonuclease Msp I (25 units) for CYP2C19*2 and Bam HI (25 unit) for CYP2C19*3 followed by electrophoresis in 3% agarose gels.

Phenotypes of CYP2C19 were predicted based on the band patterns of the polymerase chain reaction products, according to the method of Kubota et al.[13] Briefly, samples showing either CYP2C19*2 or CYP2C19*3 mutation in a homozygous state or CYP2C19*2 and CYP2C19*3 mutations in a combined heterozygous state were classified as the PM phenotype. Samples showing either CYP2C19*2 or CYP2C19*3 mutation in a heterozygous state were classified as the heterozygous EM phenotype, and those showing no CYP2C9*2 or CYP2C19*3 alleles were classified as the homozygous EM phenotype.[9,10]

Determination of Omeprazole and Its 5-Hydroxylated Metabolite in Plasma Samples

Omeprazole, the 5-hydroxy metabolite of omeprazole, and an internal standard [4,6-dimethyl-2-[(4-methoxy-2-pyridinyl)methyl]sulphinyl]-1H-benzimidazole] in plasma samples (500 µL) were extracted at pH 7.0 into ethyl acetate (1 mL).[16] A portion of the extract (150 µL) was injected onto a normal-phase liquid chromatographic column (LiChrospher Diol, 5 µm, 120 × 4.0 mm, Merck, Germany). The mobile phase consisting of 0.05% ammonium hydroxide, 0.8% water, 8% methanol, and 55% isohexane in ethyl acetate was delivered at a flow rate of 1.0 mL/min. Retention times were 3.5, 8.0, and 5.5 minutes for omeprazole, the 5-hydroxy-omeprazole, and the internal standard, respectively. The analytic compounds in the eluate were detected using a UV absorption method at 302 nm. The absolute recovery of omeprazole was greater than 90% at 25 to 2500 nmol/L, and that for 5-hydroxy metabolite was 70% at 50 to 3000 nmol/L. The limit of quantification for omeprazole and 5-hydroxyomeprazole were 25 and 50 nmol/L, respectively, with coefficients of variation (CV) of less than 20%.

Determination Plasma Cortisol and Urinary 6 -Hydroxycortisol Levels

Urinary concentrations of unconjugated 6 -HC were assayed with a high-performance liquid chromatography (HPLC) coupled with an ultraviolet (UV) absorption method according to that of Bienvenu et al, with minor modifications.[17,18] Briefly, the mobile phase consisting of mixtures of acetonitrile/water/trichloroacetic acid (8/92/0.0005 vol/vol/wt, respectively) were ad-

125

justed to pH 2.5 by phosphoric acid and used in the assay. The HPLC system consisted of a reverse phase column (Prodigy 5µODS, 150 × 4.6 mm, Phenomenex, Torrance, Calif), a pump (L-7100, Hitachi Co Ltd, Tokyo, Japan), a UV detector (UV-8000, Tosoh Co Ltd, Tokyo, Japan) set at 244 nm, and a chromato-integrator (D-7500, Hitachi). The recovery rates for 6 -HC, and the internal standards extracted from urine samples were greater than 95% with CV below 4%. Within-day and between-day CV for determining 200 and 20 ng/mL of urinary 6 -HC and cortisol were both below 5%. Plasma cortisol concentrations were assayed using a fluorescence polarization immunoassay method (TDX system, Abbott Diagnostics, South Pasadena, Calif). Samples were prepared according to the manufacturer's instruction. Within-day and between-day CV for determining 0.05 and 0.1 µg/mL cortisol were both below 5%.

Pharmacokinetic and Statistical Analyses

Partial cortisol clearance to 6 -HC ($CL_{cortisol\ 6\ -HC}$) was calculated as follows:

$$CL_{cortisol\ 6\ -HC} = [Ae_{(6\ -HC)}/3]/C_{cortisol} \text{ (Equation 1)}$$

where $Ae_{(6\ -HC)}/3$ represents the average urinary excretion rates of 6 -HC during the 3-hour urine collection period, and $C_{cortisol}$ is the plasma cortisol concentration determined at the midpoint of the urine collection period.

Equation 1 is based on the assumption that the rate of 6 -HC formation from cortisol equals the rate of appearance in urine and that 6 -HC is eliminated in the urine without further metabolism. In addition, Equation 1 is based on the assumption that the midpoint plasma cortisol concentration represents the mean plasma cortisol concentration during the urine sampling period and that collection of urine is complete. Based on these assumptions, we consider that $CL_{cortisol\ 6\ -HC}$ would represent the enzyme activity involved in the formation of 6 -HC from cortisol. This parameter has been reported and assessed previously by our group using a potent CYP3A inhibitor, clarithromycin.[18]

Data are expressed as mean ± SEM throughout the study, unless otherwise stated. The mean values for the omeprazole hydroxylation index and $CL_{cortisol\ 6\ -HC}$ between the CLD group and the control group as well as within the same group were compared statistically by multiple comparisons analysis followed by Dunnett's t test. Correlation between the above 2 indices of the in vivo metabolic activities of CYP2C19 and CYP3A and clinical characteristics and/or biochemical parameters
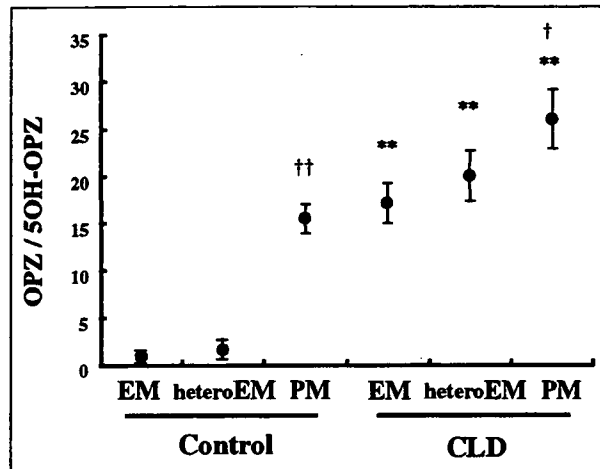

Figure 1. The mean (± SEM) of omeprazole hydroxylation index (OPZ/5OH-OPZ) in healthy subjects and patients with chronic liver disease having the respective genotypes of CYP2C19. EM = extensive metabolizers with the homozygous wild-type CYP2C19 genotype; heteroEM = heterozygous extensive metabolizer with the heterozygous CYP2C19*2 or CYP2C19*3 genotype (CYP2C19*1/*2 or *1/*3); PM = poor metabolizers with homozygous CYP2C19*2 and CYP2C19*3 (CYP2C19*2/*2 or *3-*3) or combined heterozygous CYP2C19*2 and CYP2C19*3 genotypes (CYP2C19*2/*3); OPZ/5OH-OPZ = plasma omeprazole to 5-hydroxyomeprazole ratio; CLD = chronic liver diseases (chronic hepatitis and cirrhosis). **P < .01 compared with the control subjects having the corresponding genotypes of CYP2C19. ††P < .001 compared with other genotypes (EM, heteroEM) of the control group. †P < .05 compared with EM patients with chronic liver disease.

was analyzed by multiple regression analysis (SAS version 8.2, SAS Institute, Cary, NC). A P value of <.05 was considered statistically significant.

RESULTS

Omeprazole to 5-Hydroxyomeprazole Ratio in the Controls and Patients With CLD

The 3-hour omeprazole hydroxylation index (ie, 3-hour postdose plasma concentration ratio of omeprazole/5-hydroxyomeprazole [OPZ/5OH-OPZ] ratio) has been considered to be a useful in vivo biomarker of CYP2C19 activity by many investigators.[19-22] Because the index has an inverse relationship with CYP2C19 activity, a higher index indicates lower in vivo CYP2C19 activity.

In healthy subjects with different CYP2C19 genotypes, the mean OPZ/5OH-OPZ ratio was significantly (P < .01) higher in subjects with the PM genotypes (15.5 ± 1.52) than in those with homozygous ± (0.81 ± 0.09) and heterozygous EM (1.55 ± 0.20) genotypes (Figure 1). In patients with CLD, the mean OPZ/5OH-OPZ ratio

126
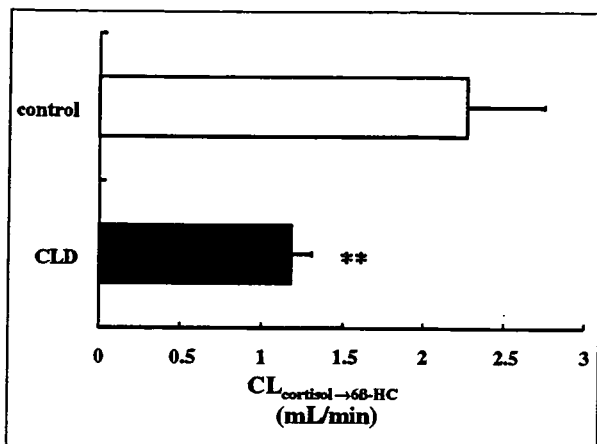
Figure 2. Partial formation clearance of cortisol to 6 - hydroxycortisol ($CL_{cortisol\ 6\ -HC}$) in patients with chronic liver disease and in control subjects. $CL_{cortisol\ 6\beta-HC}$ = partial formation clearance of cortisol to 6 -hydroxycortisol; CLD = chronic liver disease. **P < .001 compared with the control group.
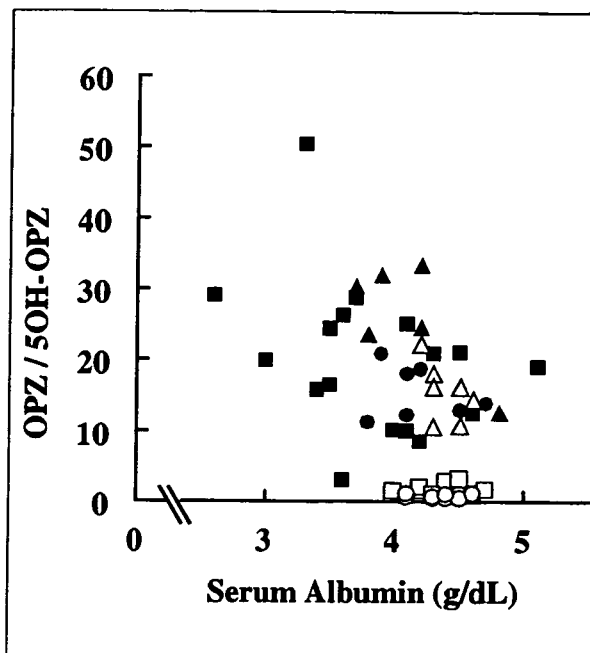

Figure 3. Relationships between omeprazole hydroxylation index (OPZ/5OH-OPZ) and serum concentrations of albumin in patients with chronic liver diseases (CLD) and the healthy control subjects having different CYP2C19 genotypes. The CLD patients with the CYP2C19 genotypes of homozygous extended metabolizer, heterozygous extended metabolizer, and poor metabolizer are denoted by closed circles (●), squares (■), and triangles(▲), respectively, and the healthy subjects having the corresponding CYP2C19 genotypes are denoted by open circles ( ), squares ( ), and triangles ( ), respectively. The relationship between serum albumin level and hydroxylation index in CLD patients and healthy subjects is statistically significant (n = 61, r = -.526, P < .001, Y = 63.5 - 12.3X). OPZ/ 5OH-OPZ = plasma omeprazole to 5-hydroxyomeprazole concentration ratio.

was significantly (P < .05) greater in patients with the PM genotypes (26.04 ± 3.15; n = 6) than in those with the homozygous EM genotype (17.15 ± 2.12; n = 7), and the ratio in those with heterozygous EM genotypes (61/ 62, n = 11; 61/63, n = 6; 20.02 ± 2.63) was in between the values of the 2 homozygous genotypes. The omeprazole hydroxylation index of patients with different CYP2C19 genotypes was significantly (P < .01) greater than that of control subjects with the corresponding genotypes.

Partial Formation Clearance of 6 -Hydroxycortisol ($CL_{cortisol\ 6\ -HC}$)

The mean value of $CL_{cortisol\ 6\ -HC}$ obtained from CLD patients was significantly (P < .001) lower than that obtained from the control group (1.19±0.12 versus 2.26 ± 0.24 mL/min) (Figure 2). In patients with CLD, the mean $CL_{cortisol\ 6\ -HC}$ decreased with an increase in severity of liver impairments as follows: 1.35 ± 0.26 in patients with chronic hepatitis and 1.12 ± 0.13 in patients with cirrhosis. The value was significantly lower (P < .05) in patients with cirrhosis compared with control subjects.

Correlations Between Omeprazole Hydroxylation Index or $CL_{cortisol\ 6\ -HC}$ and Patients' Covariates

Table 2 shows the results of multiple regression analysis between the omeprazole hydroxylation index or $CL_{cortisol\ 6\ -HC}$ and patients' covariates (ie, demographic

parameters and laboratory tests) in CLD patients and control subjects. A significant (P < .05) correlation was observed between omeprazole hydroxylation index and disease condition, serum albumin level, or CYP2C19 genotype (Table 2). On the other hand, no significant correlation was observed between $CL_{cortisol\ 6\ -HC}$ and all the variables tested, except disease condition (Table 2). There was a significant relationship between serum albumin concentration and the omeprazole hydroxylation index for overall data (n = 61, r = .526, P < .001) (Figure 3). When we analyzed the subset of CLD patients with the homozygous and heterozygous EM genotypes of CYP2C19 (ie, excluding control subjects and CLD patients with the PM genotype), the relation between serum albumin concentration and omeprazole hydroxylation index remained significant (n = 25, r = -.428, P < .05).

127